Supporting Information

A novel phase function describing light scattering of layers containing colloidal nanospheres

Junxin Wang,[a] Changgang Xu,[a,b] Annica M. Nilsson,[a] Daniel L. A. Fernandes[a] and Gunnar A. Niklasson*[a]

[a.] Department of Engineering Sciences, The Ångstrom Laboratory, Uppsala University, PO Box 534, SE-75121 Uppsala, Sweden

[b.] School of Materials Science and Engineering, Xi'an University of Science and Technology, Xi'an 710054, China

*E-mail: Gunnar.Niklasson@angstrom.uu.se

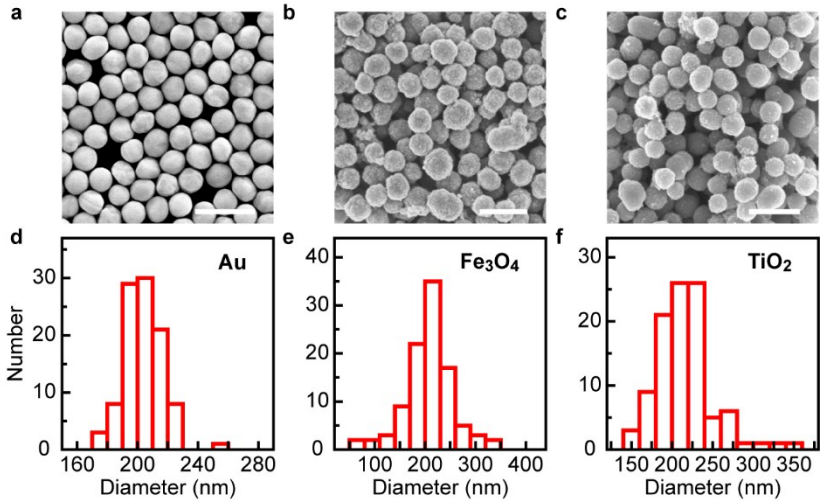

Fig. S1 Scanning electron microscope (SEM) images (upper row, scale bar: 500 nm) and corresponding diameter distributions (bottom row) for (a,d) Au, (b,e) Fe_3O_4 and (c,f) TiO_2 nanoparticles. Particle diameters were determined by Adobe Illustrator software. A hundred nanoparticles were measured to obtain the size distributions for each sample.

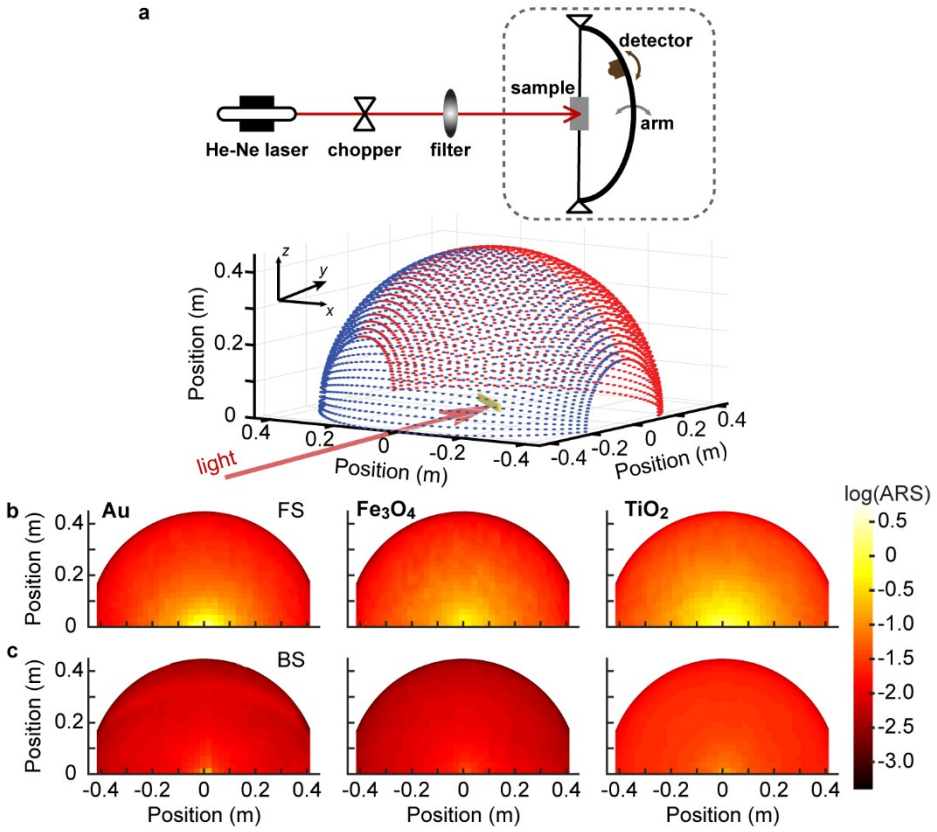

Fig. S2 Measurement positions of the 3D goniometer. (a) The 3D goniometer (upper) measures the intensity as the arm moves and the detector moves on the arm. It records the scattering in the forward (red) and backward (blue) half hemisphere (bottom) as a function of spatial detector position (x,y,z). Half hemisphere forward (b) and backward (c) scattering diagrams for Au, Fe_3O_4 and TiO_2 nanoparticles in PVP (displayed on a logarithmic scale) as a function of detector position. The incident light was from a He–Ne laser with 633 nm wavelength.

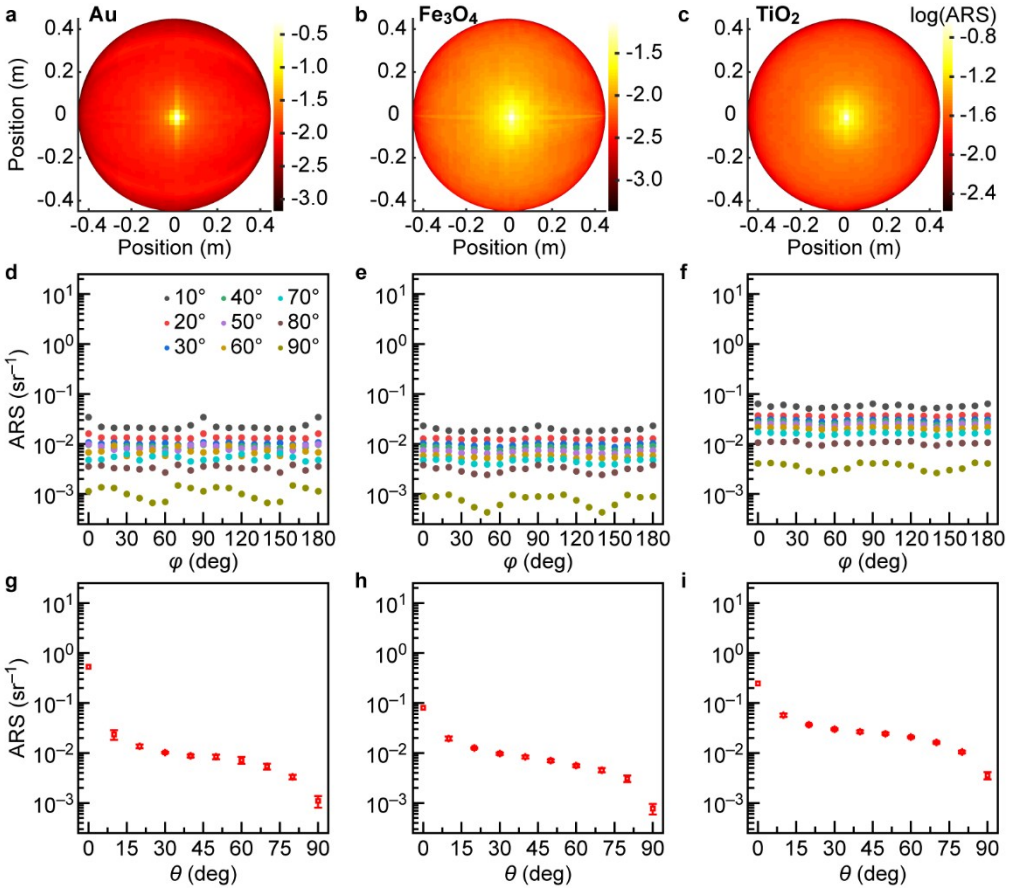

Fig. S3 (a-c) Top view of the backward ARS against position for three nanoparticle layers (in logarithmic scale). (d-f) Backward ARS as a function of azimuth angle, taken at different polar angles (inset) from 0˚ to 90˚, at an interval of 10˚. Since backward scattering is lower than the forward one, higher measurement fluctuations occur. The data do not show a significant dependence on azimuth angle. (g-i) Backward ARS plotted as a function of scattering angle, defined so that 0˚ corresponds to the direction of specular reflection. The three columns give data for Au, Fe_3O_4 and TiO_2 nanoparticle layers in PVP, respectively. The wavelength of the incident light was 633 nm.

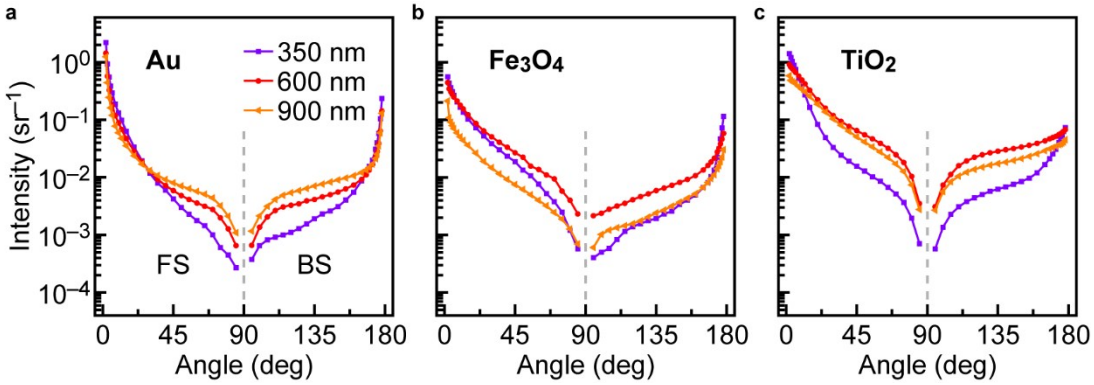

Fig. S4 Measured forward and backward ARS for Au (a), Fe_3O_4 (b) and TiO_2 (c) nanoparticles dispersed in PVP at wavelengths of 350, 600 and 900 nm as a function of polar angle.

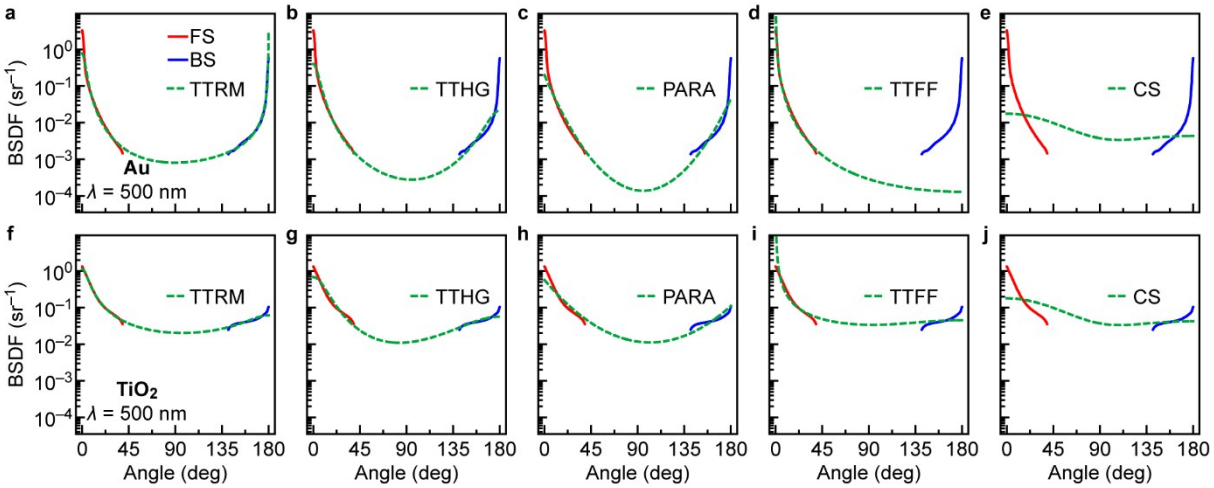

Fig. S5 Fitting of the forward and backward scattering distributions for Au (a-e) and TiO_2 (f-j) samples at a wavelength of 500 nm, with (a,f) TTRM, (b,g) TTHG, (c,h) PARA, (d,i) TTFF and (e,j), CS empirical phase functions.

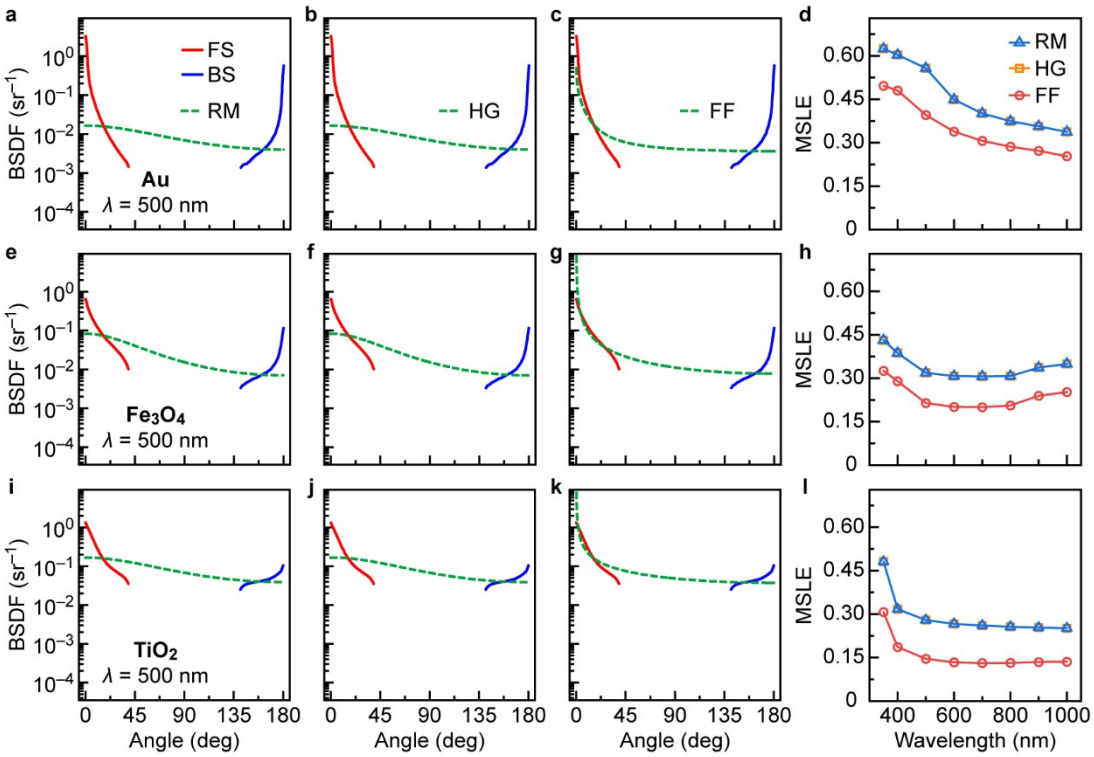

Fig. S6 Fitting of the forward and backward scattering distributions for Au (a-c), Fe_3O_4 (e-g) and TiO_2 (i-k) samples at a wavelength of 500 nm, to empirical phase functions; first column, RM, second column, HG, third column, FF. (d,h,l) Mean square logarithmic error (MSLE) of the fit to these three functions at wavelengths from 350 nm to 1000 nm (fourth column). HG and RM errors are overlapping. It is observed that the MSLE of HG, RM and FF functions are much higher than for their respective two term functions, mainly because the one-term functions fail to reproduce the backscattering peaks.

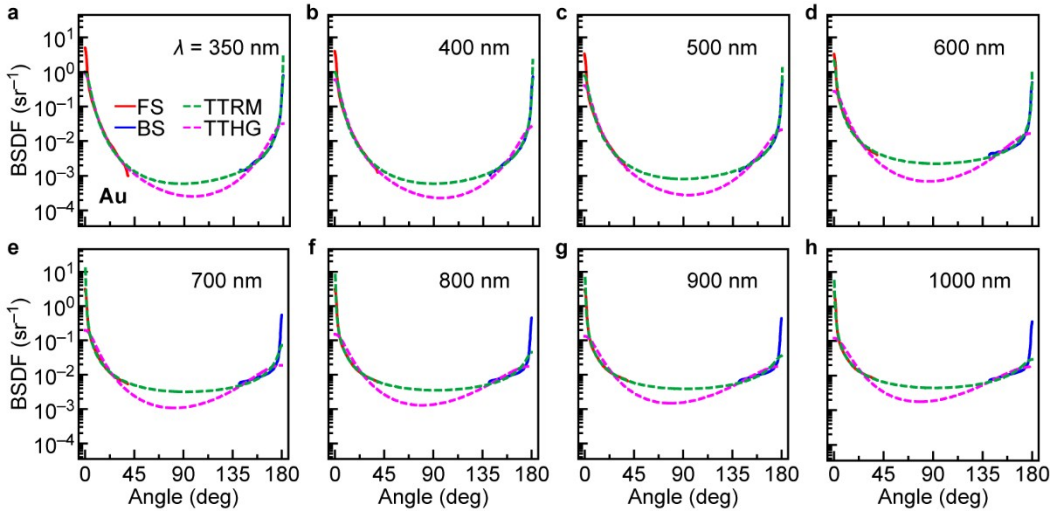

Fig. S7 Fitting of the forward and backward scattering distributions for a Au sample in the wavelength range from 350 nm to 1000 nm by use of the TTHG and TTRM phase function approximations.

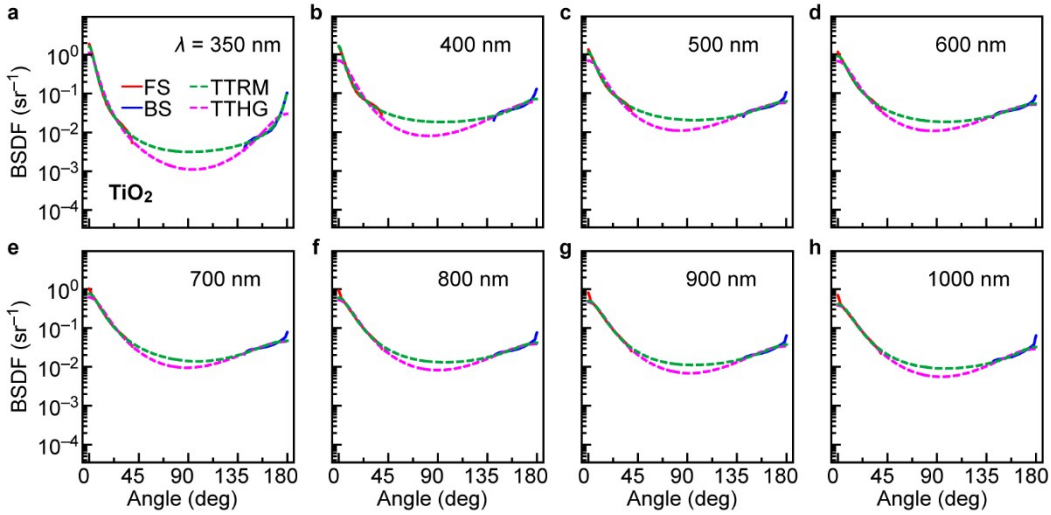

Fig. S8 Fitting of the forward and backward scattering distributions for a TiO_2 sample in the wavelength range from 350 nm to 1000 nm by use of the TTHG and TTRM phase function approximations.

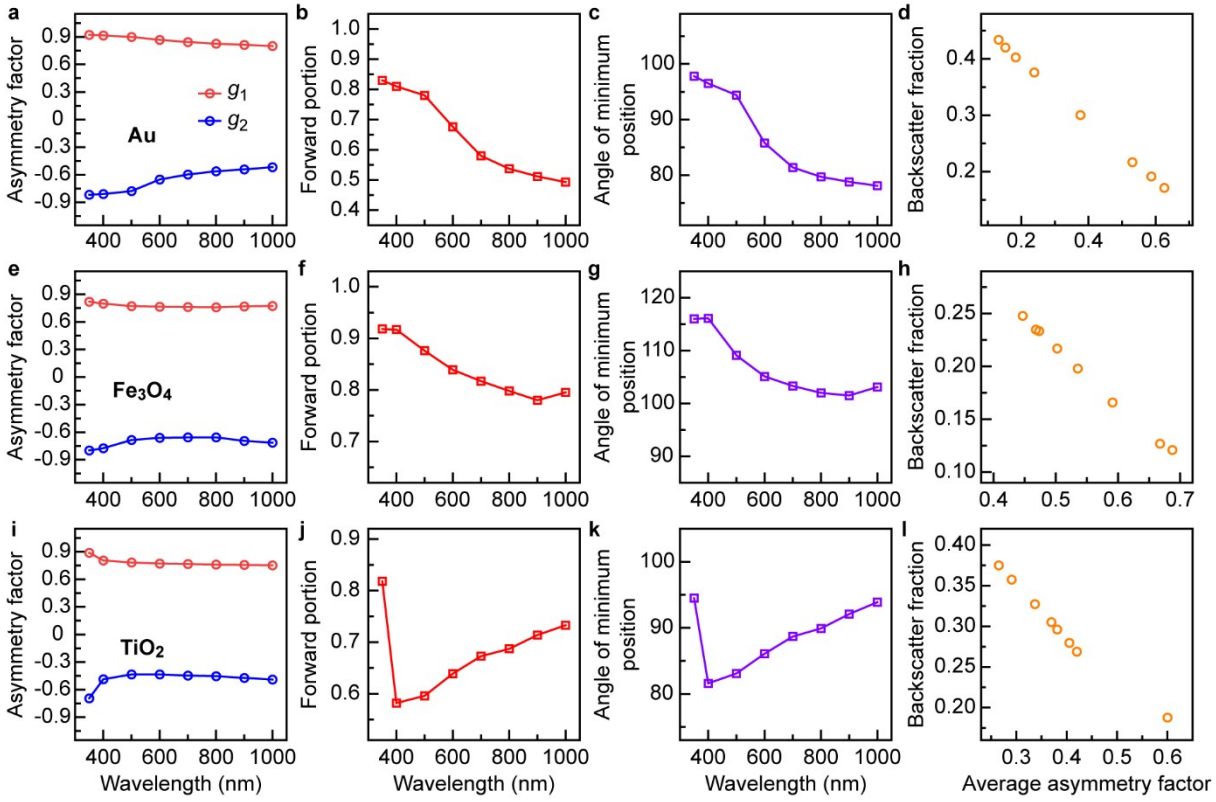

Fig. S9 Asymmetry factors g_1 and g_2 (first column), fitted forward scattering fraction, γ (second column), angle of minimum position (third column), and backscatter fraction against average asymmetry factor (fourth column) obtained by fits to the TTHG phase function of Au (a-d), Fe_3O_4 (e-h) and TiO_2 (i-l) samples at wavelengths from 350 nm to 1000 nm. Positive g represents dominant forward scattering while negative g implies dominant backscattering. Smaller absolute values of g correspond to a more diffuse scattering pattern, i.e., in Au, more diffuse forward and backward scattering happens at larger wavelengths. The parameter γ is the fitted forward scattering portion, which is larger than 0.5 indicating that forward scattering dominates (b,f,j). From the fitting, we can determine the angles related to the minimum position of the phase function (c,g,k). They exhibit a similar trend as the fitted forward portion, since higher forward scattering will push the minimum towards the backward region. The curves in (d,h,l) represent the backscatter fraction as a function of the averaged asymmetry factor $\langle g\rangle=\gamma g_1+(1-\gamma)g_2$. The backscatter fraction is equal to[1]:

$$\frac{1}{4\pi}\int_{-1}^{0}\int_{0}^{2\pi} P(\cos(\theta))d\varphi d\cos(\theta) \qquad (1)$$

A higher average asymmetry factor leads to a lower backscatter fraction as seen in (d,h,l).

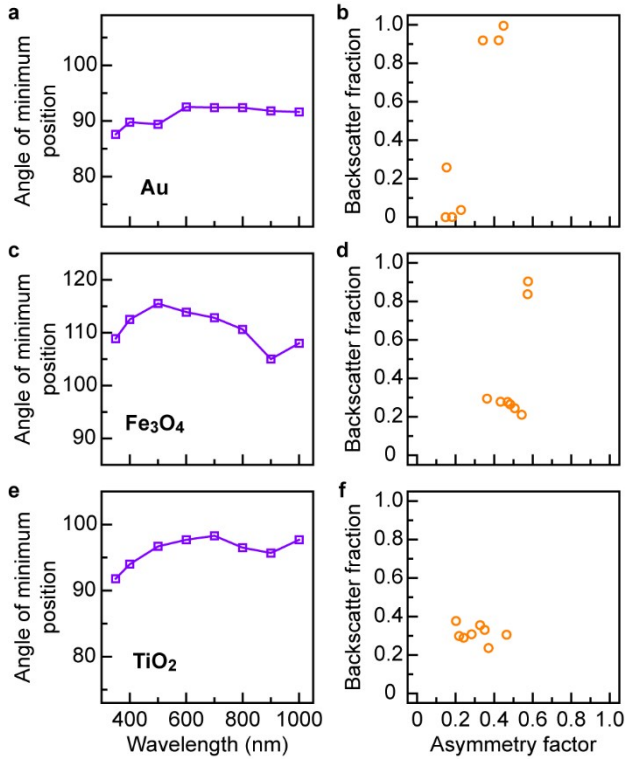

Fig. S10 Angle of minimum position (left column), and backscatter fraction against average asymmetry factor (right column) obtained from fits to the TTRM phase function of Au (a,b), Fe_3O_4 (c,d) and TiO_2 (e,f) at wavelengths from 350 nm to 1000 nm.

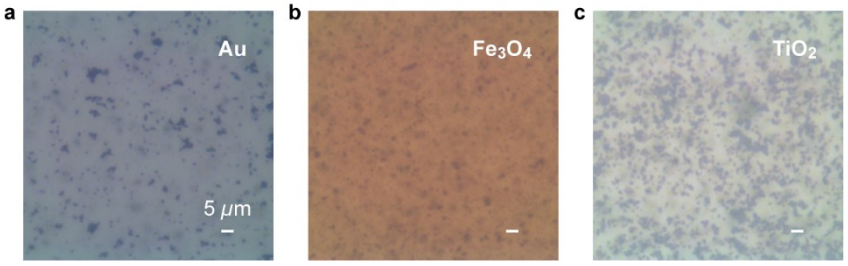

Fig. S11 Optical microscope images (50x) showing the dispersions of (a) Au, (b) Fe_3O_4 and (c) TiO_2 nanospheres in the PVP matrix. It is observed that aggregation occurs for the samples. The images show all particles within the depth of focus of the microscope.

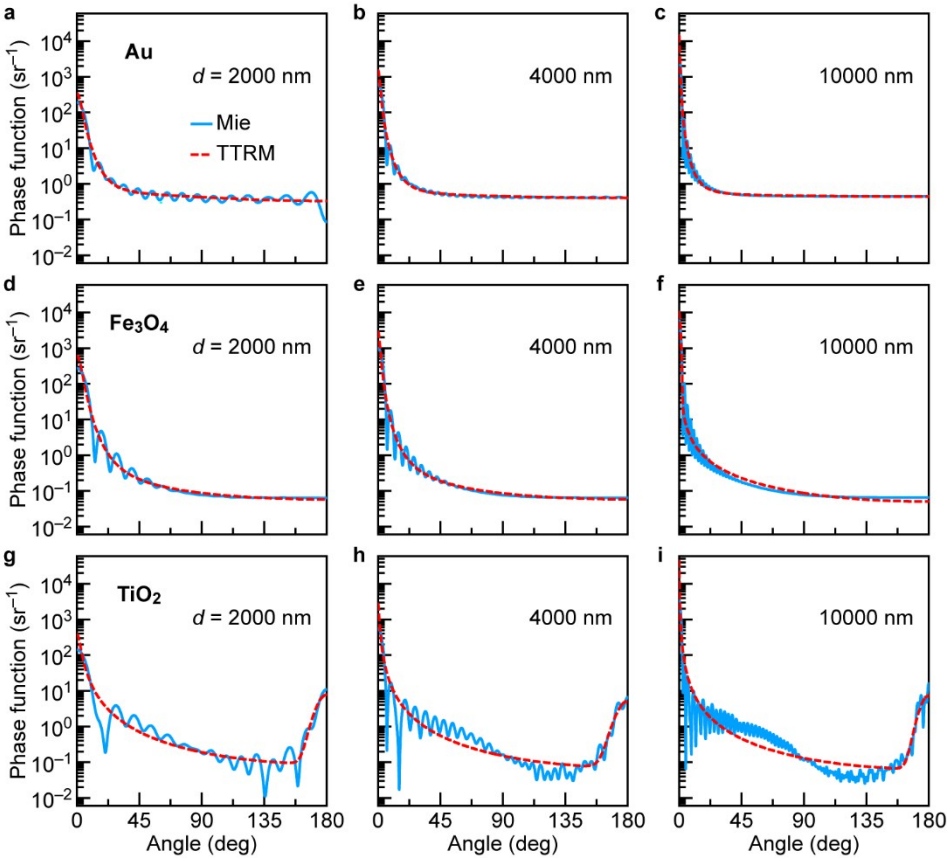

Fig. S12 Comparison of TTRM phase function (red) with the phase function computed from Mie scattering models (blue) for Au (a-c), Fe_3O_4 (d-f) and TiO_2 (g-i) nanoparticle composites at particle diameters of 2000 nm, 4000 nm and 10000 nm. The simulation was conducted at a wavelength of 600 nm.

Reference:

1. V. I. Haltrin, *Appl. Opt.*, 2002, **41**, 1022-1028.